AFRL-OSR-VA-TR-2015-0177

Collaborative Research Model Reduction for Nonlinear and Parametric Systems with Uncertainty

Matthias Heinkenschloss
WILLIAM MARSH RICE UNIV HOUSTON TX

07/14/2015
Final Report

Air Force Research Laboratory
AF Office Of Scientific Research (AFOSR)/RTA
Arlington, Virginia 22203
Air Force Materiel Command

REPORT DOCUMENTATION PAGE

Form Approved
OMB No. 0704-0188

PLEASE DO NOT RETURN YOUR FORM TO THE ABOVE ORGANIZATION.

1. REPORT DATE *(DD-MM-YYYY)*	2. REPORT TYPE	3. DATES COVERED *(From - To)*
10-07-2015	Final Report	15-April-2012 to 14-April-2015

4. TITLE AND SUBTITLE
COLLABORATIVE RESEARCH: MODEL REDUCTION FOR NONLINEAR AND PARAMETRIC SYSTEMS WITH UNCERTAINTY

5a. CONTRACT NUMBER

5b. GRANT NUMBER
FA9550-12-1-0155

5c. PROGRAM ELEMENT NUMBER

6. AUTHOR(S)
Heinkenschloss, Matthias
Sorensen, Danny, C.

5d. PROJECT NUMBER

5e. TASK NUMBER

5f. WORK UNIT NUMBER

7. PERFORMING ORGANIZATION NAME(S) AND ADDRESS(ES)
Department of Computational and Applied Mathematics - MS 134
William Marsh Rice University
6100 Main Street
Houston, Texas 77005

8. PERFORMING ORGANIZATION REPORT NUMBER

9. SPONSORING/MONITORING AGENCY NAME(S) AND ADDRESS(ES)
USAF, AFRL
AF Office of Scientific Research
875 N. Randolph Street
Arlington, VA 22203

10. SPONSOR/MONITOR'S ACRONYM(S)

11. SPONSOR/MONITOR'S REPORT NUMBER(S)

12. DISTRIBUTION/AVAILABILITY STATEMENT
Public Release distribution A

13. SUPPLEMENTARY NOTES

14. ABSTRACT

This project has developed and analyzed new mathematical algorithms to substantially reduce the complexity of simulating and optimizing parametrically dependent systems and to support decision-making under uncertainty. Specifically, this research has advanced the state of the art in reduced order modeling based on projections and on the discrete empirical interpolation method (DEIM) for nonlinear systems, developed new adaptive sampling methods for optimization of systems with uncertain inputs, devised a domain decomposition based methods to systematically integrate the uncertainty propagation through components into uncertainty propagation through a systems composed of these components, established a so-called CUR factorization based on the DEIM that provides a low rank approximate factorization of a given large matrix with applications to POD model reduction and analysis of data. The feasibility of our algorithms was demonstrated on a number of problems with relevance to the Air Force.

15. SUBJECT TERMS

16. SECURITY CLASSIFICATION OF:			17. LIMITATION OF ABSTRACT	18. NUMBER OF PAGES	19a. NAME OF RESPONSIBLE PERSON
a. REPORT	b. ABSTRACT	c. THIS PAGE			Melinda Cotten
U	U	U	UU		19b. TELEPHONE NUMBER *(Include area code)* 713-348-6200

Reset

INSTRUCTIONS FOR COMPLETING SF 298

1. REPORT DATE. Full publication date, including day, month, if available. Must cite at least the year and be Year 2000 compliant, e.g. 30-06-1998; xx-06-1998; xx-xx-1998.

2. REPORT TYPE. State the type of report, such as final, technical, interim, memorandum, master's thesis, progress, quarterly, research, special, group study, etc.

3. DATES COVERED. Indicate the time during which the work was performed and the report was written, e.g., Jun 1997 - Jun 1998; 1-10 Jun 1996; May - Nov 1998; Nov 1998.

4. TITLE. Enter title and subtitle with volume number and part number, if applicable. On classified documents, enter the title classification in parentheses.

5a. CONTRACT NUMBER. Enter all contract numbers as they appear in the report, e.g. F33615-86-C-5169.

5b. GRANT NUMBER. Enter all grant numbers as they appear in the report, e.g. AFOSR-82-1234.

5c. PROGRAM ELEMENT NUMBER. Enter all program element numbers as they appear in the report, e.g. 61101A.

5d. PROJECT NUMBER. Enter all project numbers as they appear in the report, e.g. 1F665702D1257; ILIR.

5e. TASK NUMBER. Enter all task numbers as they appear in the report, e.g. 05; RF0330201; T4112.

5f. WORK UNIT NUMBER. Enter all work unit numbers as they appear in the report, e.g. 001; AFAPL30480105.

6. AUTHOR(S). Enter name(s) of person(s) responsible for writing the report, performing the research, or credited with the content of the report. The form of entry is the last name, first name, middle initial, and additional qualifiers separated by commas, e.g. Smith, Richard, J, Jr.

7. PERFORMING ORGANIZATION NAME(S) AND ADDRESS(ES). Self-explanatory.

8. PERFORMING ORGANIZATION REPORT NUMBER. Enter all unique alphanumeric report numbers assigned by the performing organization, e.g. BRL-1234; AFWL-TR-85-4017-Vol-21-PT-2.

9. SPONSORING/MONITORING AGENCY NAME(S) AND ADDRESS(ES). Enter the name and address of the organization(s) financially responsible for and monitoring the work.

10. SPONSOR/MONITOR'S ACRONYM(S). Enter, if available, e.g. BRL, ARDEC, NADC.

11. SPONSOR/MONITOR'S REPORT NUMBER(S). Enter report number as assigned by the sponsoring/ monitoring agency, if available, e.g. BRL-TR-829; -215.

12. DISTRIBUTION/AVAILABILITY STATEMENT. Use agency-mandated availability statements to indicate the public availability or distribution limitations of the report. If additional limitations/ restrictions or special markings are indicated, follow agency authorization procedures, e.g. RD/FRD, PROPIN, ITAR, etc. Include copyright information.

13. SUPPLEMENTARY NOTES. Enter information not included elsewhere such as: prepared in cooperation with; translation of; report supersedes; old edition number, etc.

14. ABSTRACT. A brief (approximately 200 words) factual summary of the most significant information.

15. SUBJECT TERMS. Key words or phrases identifying major concepts in the report.

16. SECURITY CLASSIFICATION. Enter security classification in accordance with security classification regulations, e.g. U, C, S, etc. If this form contains classified information, stamp classification level on the top and bottom of this page.

17. LIMITATION OF ABSTRACT. This block must be completed to assign a distribution limitation to the abstract. Enter UU (Unclassified Unlimited) or SAR (Same as Report). An entry in this block is necessary if the abstract is to be limited.

COLLABORATIVE RESEARCH: MODEL REDUCTION FOR NONLINEAR AND PARAMETRIC SYSTEMS WITH UNCERTAINTY

FA9550-12-1-0155 and FA9550-12-1-0420

Matthias Heinkenschloss and Danny C. Sorensen
Department of Computational and Applied Mathematics
Rice University, Houston, Texas

Karen Willcox
Department of Aeronautics & Astronautics
Massachusetts Institute of Technology

Abstract

This project has developed and analyzed new mathematical algorithms to substantially reduce the complexity of simulating and optimizing parametrically dependent systems and to support decision-making under uncertainty. Specifically, this research has advanced the state of the art in reduced order modeling based on projections and on the discrete empirical interpolation method (DEIM) for nonlinear systems, developed new adaptive sampling methods for optimization of systems with uncertain inputs, devised a domain decomposition based methods to systematically integrate the uncertainty propagation through components into uncertainty propagation through a systems composed of these components, established a so-called CUR factorization based on the DEIM that provides a low rank approximate factorization of a given large matrix with applications to POD model reduction and analysis of data. The feasibility of our algorithms was demonstrated on a number of problems with relevance to the AirForce.

1 Introduction

Effective computational tools to support decision-making under uncertainty have become essential in the design and operation of aerospace systems. Many problems of relevance to the Air Force are described by mathematical models of high complexity—involving multiple disciplines, characterized by a large number of parameters, and impacted by multiple sources of uncertainty. The accurate and efficient propagation of uncertainties in parameters through these complex, high fidelity computational models is a significant challenge. This project has developed new mathematical algorithms and analyses to substantially reduce the complexity of simulating and optimizing parametrically dependent systems and of propagating uncertainty through systems. In particular, this research has advanced the state of the art in reduced order modeling based on projections and on the discrete empirical interpolation method (DEIM) for nonlinear systems, developed new adaptive sampling methods for optimization of systems with uncertain inputs, devised a domain decomposition based methods to systematically integrate the uncertainty propagation through components into uncertainty propagation through a systems composed of these components, established a so-

called CUR factorization based on the DEIM that provides a low rank approximate factorization of a given large matrix with applications to POD model reduction and analysis of data. The feasibility of algorithms was demonstrated on a number of problems with relevance to the AirForce. This report highlights several of our research results. More details can be found in the publications [1, 2, 3, 4, 5, 7, 8, 9, 10, 11, 13] and theses [6, 12] that resulted from this research.

Sections 2.1 to 2.4 summarize our advancements to the state of the art in reduced order modeling based on projections and on the discrete empirical interpolation method (DEIM) for nonlinear systems. Section 2.1 is concerned with the application of the Discrete Empirical Interpolation Method (DEIM) to systems obtained by finite element discretizations of partial differential equations, and to a class of parameterized system that arises, e.g., in shape optimization. Careful analysis and reorganizations of computations lead to evaluations of the DEIM reduced order models (ROMs) that are substantially faster than those of the standard projection based ROMs. Additional gains are obtained with the DEIM ROMs when one has to compute derivatives of the model with respect to the parameter.

Traditionally, projection based reduced order models use only one subspace for all parameters. To obtain an accurate ROM, this can require relatively large dimensional subspaces, and, consequently, result in a less efficient ROM. The approach in Section 2.2 divides the parameter space into regions and for each region develops a different ROM. The regions in parameter space are determined using machine learning methods in the offline computational phase via clustering. This approach can lead to significantly smaller and therefore computationally cheaper ROMs.

Section 2.3 summarizes our development of an efficient approach for a-posteriori error estimation for POD-DEIM reduced nonlinear dynamical systems. Our a-posteriori error estimator can be efficiently decomposed in an offline/online fashion and is obtained by a one dimensional auxiliary ODE during reduced simulations.

The application of the DEIM requires that a component of the system nonlinearity depends only on a few components of the vector of arguments, and it requires explicit knowledge of this dependence. If DEIM based model reduction is applied to existing codes, determining this dependency can be tedious and error prone task. Section 2.4 describes how standard techniques of automatic differentiation (AD) can be adapted to producing such a code and hence can facilitate the use of DEIM by non-experts.

The methods in sections 2.5 and 2.6 are concerned with efficient uncertainty propagation through coupled systems, and efficient optimization of PDE systems with uncertain parameters. Thus, while the methods summarized in sections 2.1 to 2.4 deal with complexity reduction in simulation of general parameterized systems, the approaches in sections 2.5 and 2.6 integrate the statistical distributions of the uncertain parameters.

We have developed a rigorous framework based on trust-region algorithms and adaptive stochastic collocation for the efficient solution of optimization problems governed by partial differential equations with uncertain parameters. Sparse grid collocation or other sampling methods lead to inexact

objective functions and gradients in the optimization problems. Our new trust-region framework rigorously manages the use of this inexact problem information. As a result, we dramatically reduce the number of samples required, which leads to a dramatic reduction in the computational cost. Moreover, numerical results indicate that our new algorithm rapidly identifies the stochastic variables that are relevant to obtaining an accurate optimal solution. When the number of such variables is independent of the dimension of the stochastic space, the algorithm exhibits near dimension-independent behavior.

Decomposition of a system into subsystems or component parts is another strategy to manage complexity. We have developed a domain decomposition approach for uncertainty analysis. Our approach sketched in Section 2.6 generates computational models for the propagation of uncertainty through the subsystems. These subsystem models are computed independently in an "offline" phase and they account for propagation of uncertainly through interface conditions, which is important for the coupled systems. Once the subdomain models are constructed, importance sampling is used to couple the subdomain models and analyze the propagation of uncertainty in the global system. This last step is performed in an"online" phase and does not require expensive simulations.

Finally, Section 2.7 summarizes our development and analyzes of a new CUR matrix factorization for matrices built from large-scale data sets. The CUR offers two advantages over the SVD: when the data in **A** are sparse, so too are the **C** and **R** matrices, unlike the matrices of singular vectors; and the columns and rows that comprise **C** and **R** are representative of the data (e.g., sparse, nonnegative, integer valued, etc.). Our algorithm is novel in that it only requires *one pass* through the data **A** and only requires a few columns of **A** to be in memory at any given step of the algorithm. This is ideal for POD based model reduction schemes since the high dimensional trajectory need not be stored.

2 Accomplishments

This rsection highlights several of our research results. More details can be found in the publications [1, 2, 3, 4, 5, 7, 8, 9, 10, 11, 13] and theses [6, 12] that resulted from this research.

2.1 Application of the Discrete Empirical Interpolation Method to Reduced Order Modeling of Nonlinear and Parametric Systems

Projection based methods lead to reduced order models (ROMs) with dramatically reduced numbers of equations and unknowns. However, for nonlinear or parametrically varying problems the cost of evaluating these ROMs still depends on the size of the full order model and therefore is still expensive. The Discrete Empirical Interpolation Method (DEIM) further approximates the

nonlinearity in the projection based ROM. The resulting DEIM ROM nonlinearity depends only on a few components of the original nonlinearity. If each component of the original nonlinearity depends only on a few components of the argument, the resulting DEIM ROM can be evaluated efficiently at a cost that is independent of the size of the original problem. For systems obtained from finite difference approximations, the *i*th component of the original nonlinearity often depends only on the *i*th component of the argument. This is different for systems obtained using finite element methods, where the dependence is determined by the mesh and by the polynomial degree of the finite element subspaces. Our paper [AHS13] describes two approaches of applying DEIM in the finite element context, one applied to the assembled and the other to the unassembled form of the nonlinearity. We carefully examine how the DEIM is applied in each case, and the substantial efficiency gains obtained by the DEIM. In addition, we demonstrate how to apply DEIM to obtain ROMs for a class of parameterized system that arises, e.g., in shape optimization. The evaluations of the DEIM ROMs are substantially faster than those of the standard projection based ROMs. Additional gains are obtained with the DEIM ROMs when one has to compute derivatives of the model with respect to the parameter.

The following example is a semillinear elliptic reaction-advection-diffusion partial differential equation (PDE) posed on $\Omega = (0,18) \times (0,9) \times (0,9)$. A concentration of $u = 0.2$ is imposed on $\{0\} \times [3,6] \times \times [3,6]$. We want to represent the concentration (the solution of the semillinear elliptic PDE) for varying parameter $(\ln(A), E)$ in the reaction term. A finite element mesh (Mesh 2) of the domain Ω and concentration corresponding to parameter $(\ln(A), E) = (6.4, 0.11)$ are shown in Figure 1.

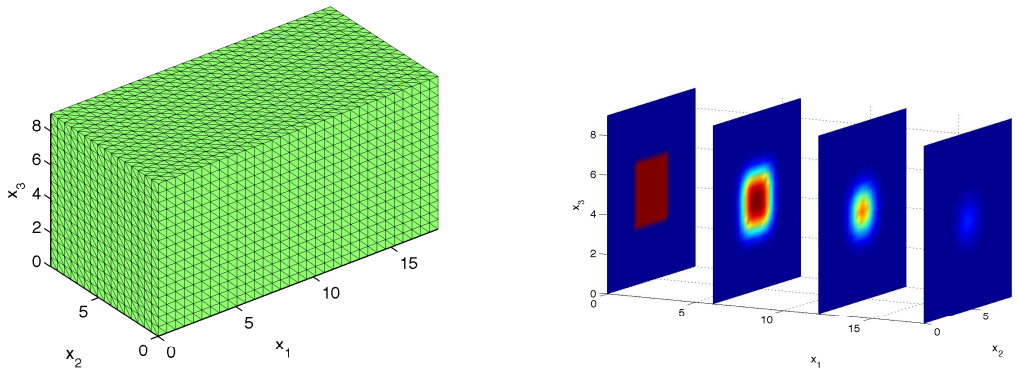

Figure 1: Coarse finite element mesh of the domain Ω (left plot) and solution of the semillinear reaction-advection-diffusion PDE with parameter $(\ln(A), E) = (6.4, 0.11)$ (right plot).

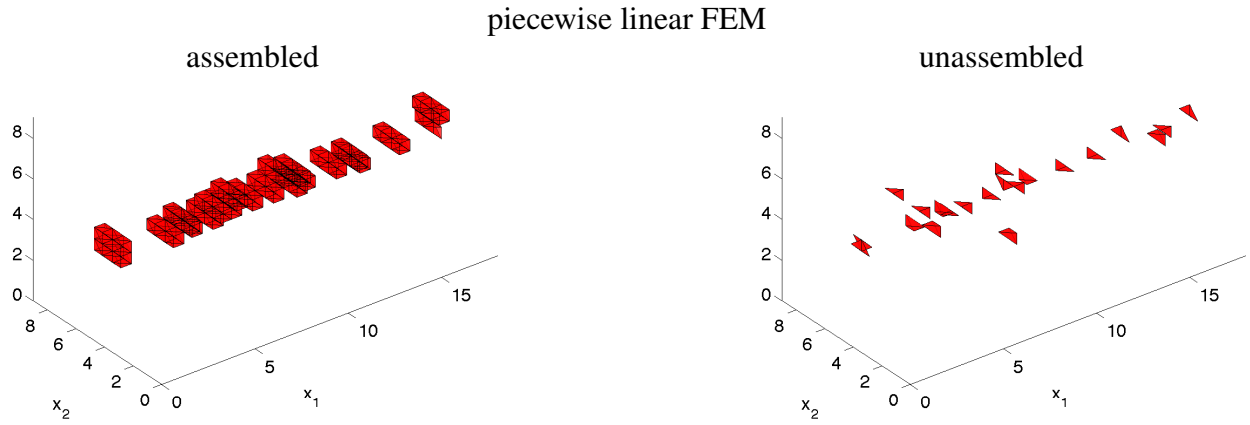

Figure 2: The tetrahedra that contain DEIM points for piecewise linear finite elements are shown.

Figure 2 shows the tetrahedra in Mesh 2 that contain a node corresponding to a DEIM point. The plots in the left column correspond to the DEIM applied to the assembled form of the nonlinearity. The expense of evaluating the DEIM reduced order model is proportional to the number of nodes the DEIM indices are connected to. Figure 2 already indicates that the unassembled form of DEIM is more efficient. This is confirmed by the timing results in Table 1. Table 1 clearly show the time saving of DEIM-POD receded order models over naive POD reduced order model for both piecewise linear ($p = 1$) and piecewise quadratic ($p = 2$) finite elements. Using the unassembled form of DEIM leads to additional gains.

Polynomial degree	$p = 1$			$p = 2$	
Mesh number	1	2	3	1	2
Full	1.78 (4)	10.60 (3)	43.30 (3)	7.80 (3)	185.00 (3)
POD	1.28 (4)	8.04 (3)	23.80 (3)	4.12 (3)	38.80 (3)
POD-DEIM	0.15 (4)	0.10 (3)	0.21 (4)	0.21 (3)	0.40 (3)
POD-DEIM-u	0.16 (9)	0.07 (4)	0.10 (4)	0.01 (4)	0.18 (4)

Table 1: The computing times (in sec) and the number of Newton iterations (in parenthesis) needed to solve the full order model, the POD reduced order model, the POD-DEIM reduced order model, and the POD-DEIM-u (unassembled) reduced order model for different grid levels and linear ($p = 1$) and quadratic ($p = 2$) finite elements.

2.2 Localized DEIM

We have proposed the Localized DEIM (LDEIM) as way to improve the efficiency of DEIM ROMs for nonlinear parameterized PDEs [PBWB13]. Whereas DEIM projects the nonlinear term onto

one global subspace, our LDEIM method computes k local subspaces, each tailored to a particular region of characteristic system behavior. Then, depending on the current state of the system, LDEIM selects an appropriate local subspace for the approximation of the nonlinear term. In this way, the dimensions of the local DEIM subspaces, and thus the computational costs, remain low even though the system might exhibit a wide range of behaviors as it passes through different regimes. LDEIM uses machine learning methods in the offline computational phase to discover these regions via clustering. In our implementation, the snapshots are clustered with k-means. Local DEIM approximations are then computed for each cluster. In the online computational phase, machine-learning-based classification procedures select one of these local subspaces adaptively as the computation proceeds. We use a nearest neighbor classifier. The classification can be achieved using either the system parameters or a low-dimensional representation of the current state of the system obtained via feature extraction.

The LDEIM approach is demonstrated for a reacting flow example of a premixed H_2-Air flame. The physics are modeled with the one-step reaction mechanism

$$2H_2 + O_2 \rightarrow 2H_2O\,,$$

where H_2 is the fuel, O_2 is the oxidizer, and H_2O is the product. The evolution of the flame in the domain Ω is given by the nonlinear advection-diffusion-reaction equation

$$\kappa\Delta\mathbf{y} - w\nabla\mathbf{y} + \mathbf{f}(\mathbf{y},\mu) = 0\,, \tag{1}$$

where $\mathbf{y} = [y_{H_2}, y_{O_2}, y_{H_2O}, T]^T$ contains the mass fractions of species H_2, O_2, and H_2O and the temperature. The constants $\kappa = 2.0\text{cm}^2/\text{sec}$ and $w = 50\text{cm/sec}$ are the molecular diffusivity and the velocity of the velocity field in x_1 direction, respectively. The geometry of the problem is shown in Figure 3. We prescribe homogeneous Dirichlet boundary conditions on the mass fractions on Γ_1 and Γ_3, and homogeneous Neumann conditions on temperature and mass fractions on Γ_4, Γ_5, and Γ_6. We have Dirichlet conditions on Γ_2 with $y_{H_2} = 0.0282, y_{O_2} = 0.2259, y_{H_2O} = 0, y_T = 950\text{K}$, and on Γ_1, Γ_3 with $y_T = 300\text{K}$.

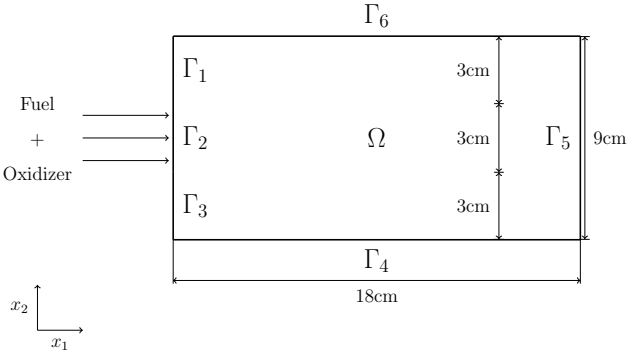

Figure 3: The spatial domain of the reacting flow simulation.

The nonlinear reaction source term $\mathbf{f}(\mathbf{y},\mu = [f_{H_2}(\mathbf{y},\mu), f_{O_2}(\mathbf{y},\mu), f_{H_2O}(\mathbf{y},\mu), f_T(\mathbf{y},\mu)]^T$ in (1) has

the components

$$\begin{aligned} f_i(\mathbf{y},\mu) &= -\nu_i\,(\eta_{H_2} y_{H_2})^2\,(\eta_{O_2} y_{O_2})\,\mu_1 \exp\left(-\frac{\mu_2}{RT}\right), \quad i = H_2, O_2, H_2O \\ f_T(\mathbf{y},\mu) &= Q f_{H_2O}(\mathbf{y},\mu), \end{aligned}$$

where ν_i and η_i are constant parameters, $R = 8.314472$J/(mol K) is the universal gas constant, and $Q = 9800$K is the heat of reaction. The parameters $\mu = (\mu_1, \mu_2) \in \mathcal{D}$ with $\mathcal{D} = [5.5\text{e+}11, 1.5\text{e+}03] \times [1.5\text{e+}13, 9.5\text{e+}03]$ are the pre-exponential factor and the activation energy, respectively. The equation (1) is discretized using the finite difference method on a 73×37 grid leading to $\mathcal{N} = 10,804$ degrees of freedom. The resulting nonlinear system of equations is solved with the Newton method. The snapshots are computed for the parameters on a 50×50 equidistant grid in $\mathcal{D}$.

Figure 4 compares DEIM, parameter-based LDEIM with splitting and clustering, and state-based LDEIM. For splitting, we set the tolerance ε to 1e-08, which is about two orders below what DEIM achieves. For the parameter-based LDEIM with clustering, the number of clusters is set to 5. More clusters lead to an unstable behavior. For the state-based LDEIM, however, we set the number of clusters to 15. The state-based LDEIM uses a point-based feature extraction with $\tilde{M} = 5$ dimensions. In all cases, we have 40 POD modes. In Figure 4, we see that the results of the parameter-based LDEIM with clustering do not improve after about 10 DEIM modes. Again, the clustering becomes unstable. However, this is not the case for state-based LDEIM which achieves about two orders of magnitude better accuracy than DEIM. The same holds for the splitting approach.

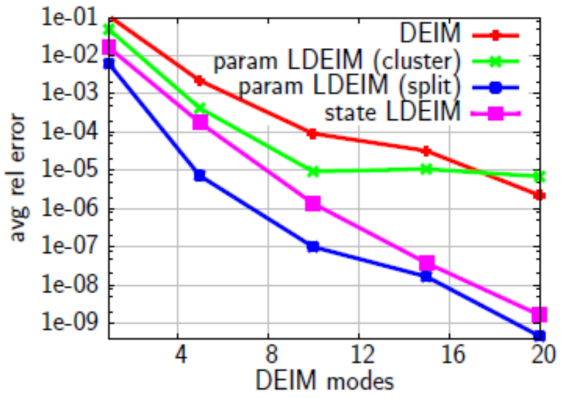

Figure 4: For the reacting flow example, the comparison between DEIM, parameter-based LDEIM, and state-based LDEIM. The results are shown for 40 POD and 20 DEIM modes. State-based LDEIM achieves about two orders of magnitude better accuracy than DEIM for the same number of DEIM modes.

2.3 A-Posteriori Error Estimation for DEIM

We have introduced an efficient approach for a-posteriori error estimation for POD-DEIM reduced nonlinear dynamical systems [WSH12]. The considered nonlinear systems may also include time and parameter-affine linear terms as well as parametrically dependent inputs and outputs. The reduction process involves a Galerkin projection of the full system and approximation of the system's nonlinearity by the DEIM method [Chaturantabut & Sorensen (2010)]. The proposed a-posteriori error estimator can be efficiently decomposed in an offline/online fashion and is obtained by a one dimensional auxiliary ODE during reduced simulations. Key elements for efficient online computation are partial similarity transformations and matrix DEIM approximations of the nonlinearity Jacobians. The theoretical results are illustrated by application to an unsteady Burgers equation and a cell apoptosis model.

The key ideas of our error estimation procedure is an application of a Gronwall-like differential inequality for the error norm $\|\mathbf{y}(t)-\mathbf{y}_r(t)\|$ (full vs. reduced state) , estimation of local logarithmic Lipschitz constants and an estimation of the DEIM approximation error for a ROM of order m using a higher order DEIM approximation of order $m+m'$. Essentially, we treat the higher order approximation heuristically as representing the true state. We use these tools to provide a-posteriori error bounds which can be computed along with the reduced system trajectory at negligible cost. Only a simple 1D ODE must be propagated along with the reduced state calculation.

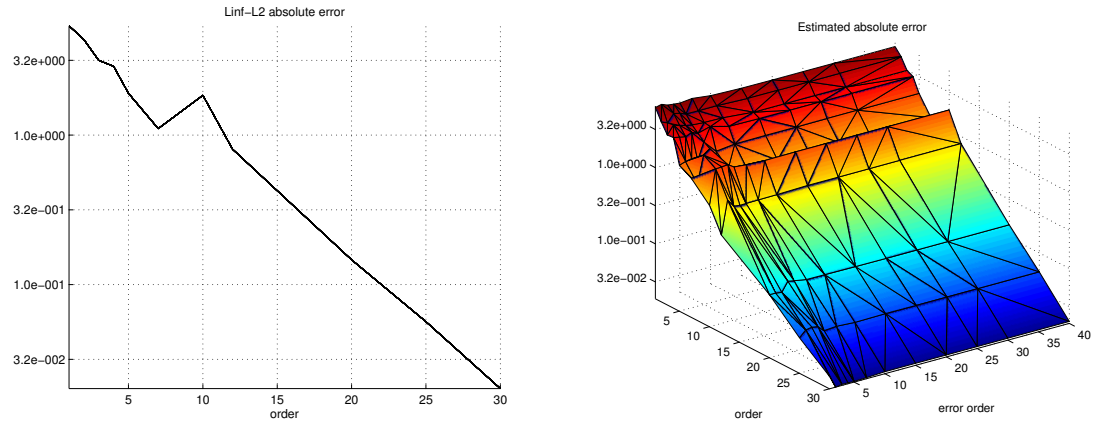

Figure 5: (Left) Absolute error of DEIM Approximation (Right) Demonstration of Error Estimate for varying m and m'

The graphs in Figure 6 illustrate the effectiveness of our error estimator. The graph on the left shows the absolute error of the reduced state from the DEIM reduced model with the true state. The right graph is a surface plot showing the error estimate using the $m+m'$ model in place of the true state. The axis labeled "order" shows the error as the model order m is increased. The axis labeled "error order" shows the estimated error as m' increases. The fact that the surface quickly flattens out in the m' direction verifies that m' does not need to be large, it typically adequate for

accurate error estimation at values between 5 and 10. This plot is for a 1D Burgers' equation but we obtained virtually identical behavior for a 60,000 variable 2D Reaction-Diffusion model Cell Apoptosis.

2.4 Automating DEIM

As mentioned previously, the Discrete Empirical Interpolation Method (DEIM) is based upon a modification to proper orthogonal decomposition which is designed to reduce the computational complexity for evaluating the reduced order nonlinear term. The DEIM approach is based upon an interpolatory projection and only requires evaluation of a few selected components of the original nonlinear term. Thus, implementation of the reduced order nonlinear term requires a new code to be derived from the original code for evaluating the nonlinearity. We have developed a methodology for automatically deriving a code for the reduced order nonlinearity directly from the original nonlinear code. The methodology is an adaptation of standard techniques of automatic differentiation (AD). This capability removes the possibly tedious and error prone task of producing such a code by hand and hence can facilitate the use of DEIM by non-experts.

We have a working prototype system that establishes proof of concept [CS12]. We were able to automatically produce a reduced order code from the original code for 2-phase miscible flow simulation. This automatically derived code was able to completely reproduce the simulation results from the hand coded ROM with essentially no degradation in computation time. The idea is to first obtain a computational graph representation of the original code and then this graph is "pruned" to retain only the graph necessary to compute the code to evaluate the DEIM selected nodes (which correspond to the DEIM indices of the desired components of the nonlinearity). The pruned graph is then used in a reverse process to generate the code for the ROM. Using standard AD techniques, one could also generate the Jacobian of the ROM automatically.

2.5 Trust-Region Algorithms with Adaptive Stochastic Collocation for PDE Optimization under Uncertainty.

We have improved our trust-region adaptive sparse grid framework for the solution of optimization problems governed by partial differential equations (PDEs) with random coefficients. While previously adaptive sparse grids were only used to generate the models used to commute the step inside the trust-region framework [7], we now also allow the approximation of function values using adaptive sparse grids [8]. This results in substantial computational savings. With our algorithmic improvements, numerical solutions that previously required high performance parallel computers[1] can now be run on a desktop [8].

[1]The computations in [7] were carried out on RedSky, an institutional computing cluster at Sandia National Laboratories. The cluster is built on a 3D toroidal QDR InfiniBand interconnect and provides 2,816 compute nodes, each with 8 cores, 2.93 GHz Nehalem X5570 processors, and 12 GB RAM per compute node.

The numerical solution of optimization problems governed by PDEs with random coefficients potentially requires a the large number of deterministic PDE solves at each optimization iteration. Our algorithm for solving such problems based on a combination of adaptive sparse-grid collocation for the discretization of the PDE in the stochastic space and a trust-region framework for optimization and fidelity management of the stochastic discretization. The overall algorithm adapts the collocation points based on the progress of the optimization algorithm and the impact of the random variables on the solution of the optimization problem. It frequently uses few collocation points initially and increases the number of collocation points only as necessary, thereby keeping the number of deterministic PDE solves low while guaranteeing convergence. Our trust-region framework now allows adaptation to build the model, as well as to approximate the objective function [8]. Our trust-region framework can be used in a wide range of applications, and extends the state-of-the-art in trust region methods for problems with inexact function and derivative information. Currently an error indicator is used to estimate gradient errors due to adaptive stochastic collocation, but other adaptive discretizations could be used as well.

The following example is motivated by the optimal control of direct field acoustic testing (DFAT). An important objective in DFAT is to accurately shape sound pressure fields in a region of interest by using acoustic sources, such as loudspeakers, located away from and directed at the region of interest. When the refractive index of the medium in the region of interest is random, we may assume that the governing physics are modeled by the stochastic Helmholtz equation

$$-\Delta u(y,x) - k^2(1+\sigma\varepsilon(y,x))^2 u(y,x) = z(x) \qquad \forall\,(y,x) \in \Gamma \times D \tag{2}$$

with Robin boundary conditions $\frac{\partial}{\partial n}u(y,x) = iku(y,x)$ for all $(y,x) \in \Gamma \times \partial D$. Here x is the spatial variable in the spatial domain D and y is the random variable. We consider an idealized DFAT example in two spatial dimensions, where the domain is $D = (-5,5)^2$. The goal of this control problem is to match the wave pressure u to a desired wave pressure $\bar{w} \in L^2(D;\mathbb{C})$ in the disk $D_R = \{x \in D \,:\, \|x\|_2 \leq R\} \subset D$. We apply distributed controls in D_C, which is the union of the regions occupied by 20 loudspeakers arranged in a circle exterior to D_R. Figure 6 depicts the experimental setup.

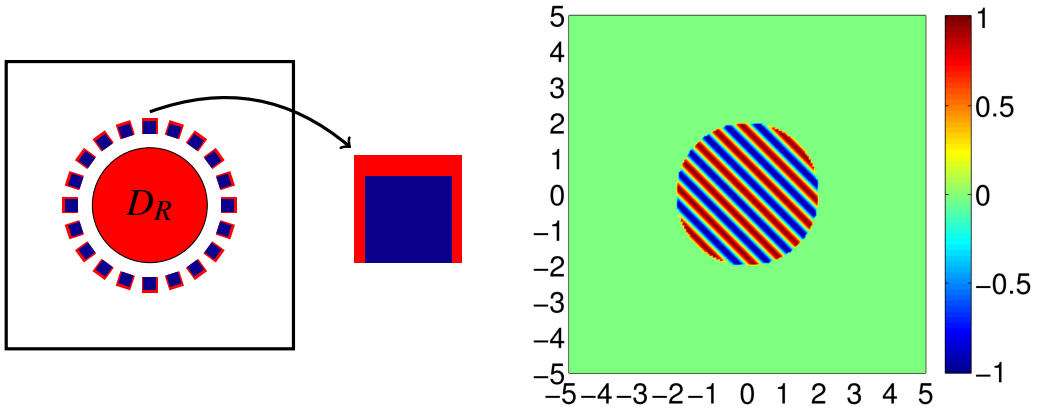

Figure 6: *Left:* A sketch of the computational domain with the region of interest D_R and 20 loudspeakers spaced uniformly along a circle surrounding D_R. The red (lighter) color denotes uncertainty in the refraction index inside D_R and uncertainty in the loudspeaker enclosures (including thickness and sound speed). The blue (darker) color stands for the loudspeaker control regions, whose union is denoted by D_C. *Right:* The real component of the desired state, $\bar{w}$.

In this example we study three sources of uncertainty: refractive index, loudspeaker thickness, and speed of sound in each loudspeaker. We assume that the stochastic refractive index is of the form $\varepsilon(y,x) = \sum_{m=1}^{M} \varepsilon_m(x) y_m$ and that its covariance is given by a Matérn covariance functions. The series representation of ε is motivated by a truncated Karhunen-Loéve (KL) expansion. In total, we have $dim = 40 + M$ random variables, 40 random loudspeaker parameters (enclosure thicknesses and wave number for each speaker) and M random variables representing the stochastic refractive index ε. For additional details see Section 5.2 in [KHRW14]. Figure 7 shows the optimal solution for ($dim = 60$ random variables (i.e., $M = 20$).

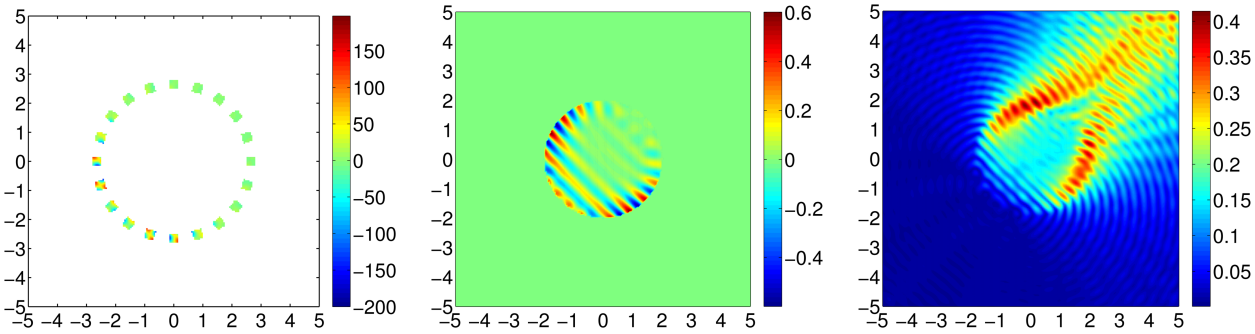

Figure 7: *Left:* The real parts of the computed optimal controls. *Center:* The real part of the expected value of the optimal state, restricted to the region of interest. *Right:* The real part of the standard deviation of the optimal state.

Table 2 gives the computational cost of our algorithm as the stochastic dimension increases from $dim = 42$ to $dim = 80$ and it illustrates the power of our algorithm. Even for the largest dimension, $dim = 80$, the problem can now be solved using a desktop. In contrast, the 40-dimensional problem using the previous version of our algorithm [KHRW13] required $1,804,001$ collocation points for the evaluation of the high-fidelity objective function, while the 80-dimensional problem now requires only 311 points due to the adaptive objective function evaluations. We also note that in this example many of the random variables are not important for the optimization context. However, it is not clear which one are the important ones. Our algorithm is able to automatically detect the important random variables and automatically zooms in on approximately 10 (out of 80) stochastic dimensions that are relevant to achieving objective function and gradient consistency conditions required by the trust-region framework. As a result it vastly reduces the effective problem size and, in this example, shows a convergence behavior that is nearly independent of the stochastic dimension.

dim	PDE Solves	CP_{obj}	CP_{grad}	Obj. Value
42	11,543	145	145	5.2542
44	32,739	233	481	5.2637
46	60,617	243	1,453	5.2641
48	79,221	247	2,961	5.2641
50	90,157	251	4,569	5.2641
60	100,911	271	7,621	5.2641
70	103,979	291	8,233	5.2641
80	105,607	311	8,253	5.2641

Table 2: Computational cost of the fully adaptive trust-region algorithm applied to the Helmholtz control example. Here *dim* is the stochastic dimension, PDE Solves is the total number of forward and adjoint PDE solves, CP_{obj} is the final number of collocation points used by the adaptive objective function scheme, CP_{grad} is the final number of collocation points used by the adaptive subproblem (gradient) model, and Obj. Value is the computed value of the objective function at termination.

2.6 A Domain-Decomposition Approach for Uncertainty Analysis.

We have proposed a new decomposition approach for uncertainty analysis of systems governed by PDEs [LW14]. The system is split into local components using domain decomposition. Our domain-decomposed uncertainty quantification (DDUQ) approach performs uncertainty analysis independently on each local component in an "offline" phase, and then assembles global uncertainty analysis results using pre-computed local information in an "online" phase. At the heart of the DDUQ approach is importance sampling, which weights the pre-computed local PDE solutions appropriately so as to satisfy the domain decomposition coupling conditions. To avoid global PDE solves in the online phase, a proper orthogonal decomposition reduced model provides an efficient approximate representation of the coupling functions.

The DDUQ approach comprises the following three steps: (1) pre-step: generate POD basis for interface functions; (2) offline step: generate local solution samples and construct surrogates for the coupling functions; (3) online step: estimate target input PDFs using surrogates and re-weight output samples. The pre-step is cheap, since although it performs standard domain decomposition iterations, the number of input samples is small. In the offline stage, expensive computational tasks are fully decomposed into subdomains, i.e., there is no data exchange between subdomains. The online stage is relatively cheap, since no PDE solve is required. This approach is summarized in Figure 8, where communication refers to data exchange between subdomains.

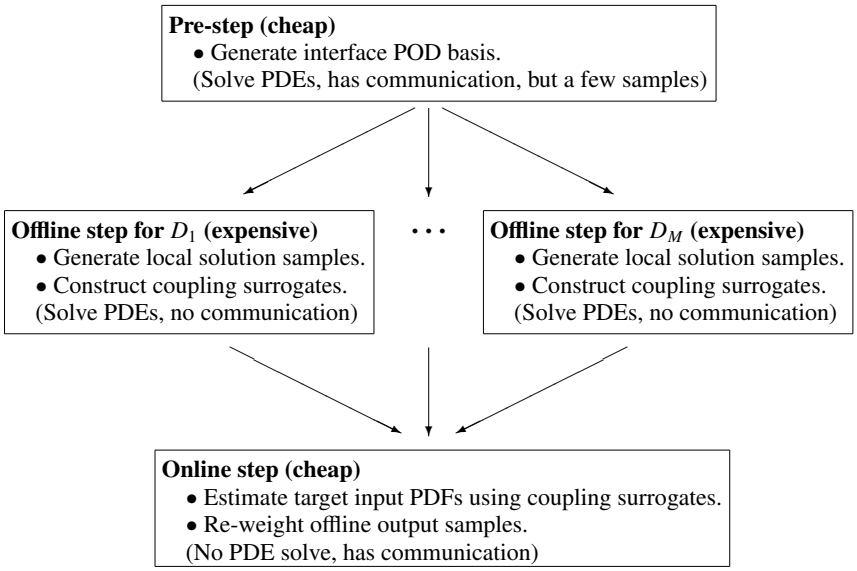

Figure 8: Domain-decomposed uncertainty quantification (DDUQ) summary.

In the offline stage of DDUQ, we first specify a proposal input PDF from which the samples will be drawn. We denote the proposal input PDF by $p_{\xi_i,\tau_i}(\xi_i,\tau_i)$, where ξ_i is the vector of uncertain parameters corresponding to subdomain i and τ_i is the vector of interface parameters for subdomain i. The proposal input PDF must be chosen so that its support is large enough to cover the support of the true (unknown) interface parameters. Provided this condition on the support is met, any proposal input PDF can be used; however, the better the proposal (in the sense that it generates sufficient samples over the support of the target input PDF) the better the performance of the importance sampling. A poor choice of proposal input PDF will lead to many wasted samples (i.e., requiring many local PDE solves).

The next step, still in the offline phase, is to perform uncertainty quantification on each local subdomain i independently. This involves generating a large number N_i of samples $\{(\xi_i^{(s)},\tau_i^{(s)})\}_{s=1}^{N_i}$ of $p_{\xi_i,\tau_i}(\xi_i,\tau_i)$, where the superscript (s) denotes the sth sample, and computing the local solutions $\{u(x,\xi_i^{(s)},\tau_i^{(s)})\}$ by solving the deterministic problem for each sample. Once the local solutions are

computed, we evaluate the local outputs of interest $\{y_i(u(x,\xi_i^{(s)},\tau_i^{(s)}))\}$ and store them.

In the online stage of DDUQ, we first generate N_{on} samples, $\{\xi^{(s)}\}_{s=1}^{N_{\text{on}}}$, of the joint PDF of inputs $\pi_\xi(\xi)$. For each sample $\xi^{(s)}$, we use the domain decomposition iteration to evaluate the corresponding interface parameters. After the above process, we have obtained a set of samples drawn from each local target input PDF $\pi_{\xi_i,\tau_i}(\xi_i,\tau_i)$. We next estimate each local target input PDF from the samples using a density estimation technique, such as kernel density estimation (KDE).

The final step of the DDUQ online stage is to use importance sampling to re-weight the outputs $\left\{y_i\left(u\left(x,\xi_i^{(s)},\tau_i^{(s)}\right)\right)\right\}_{s=1}^{N_i}$ that we generated by PDE solves in the offline stage. The weights, $w_i^{(s)}$, are computed by taking the ratio of the estimated target PDF to the proposal PDF for each local subdomain:

$$w_i^{(s)} = \frac{\hat{\pi}_{\xi_i,\tau_i}\left(\xi_i^{(s)},\tau_i^{(s)}\right)}{p_{\xi_i,\tau_i}\left(\xi_i^{(s)},\tau_i^{(s)}\right)}, \quad s=1,\ldots,N_i, \quad i=1,\ldots,M.$$

We can show that the probability computed from these weighted samples $\left\{w_i^{(s)} y_i\left(u\left(x,\xi_i^{(s)},\tau_i^{(s)}\right)\right)\right\}_{s=1}^{N_i}$ is consistent with the actual distributions of the outputs, so that under certain conditions.

We illustrate the DDUQ approach using a diffusion problem posed on a 2D spatial domain with two subdomains with randomness in the permeability coefficient, the Robin coefficient, and the source function. The PDFs of the outputs of this problem are shown in Figure 9, where we see that as the number of offline samples N_{off} increases the PDFs generated by DDUQ approach the reference PDFs (generated using the system-level Monte Carlo simulation with $N_{\text{ref}} = 10^6$ samples).

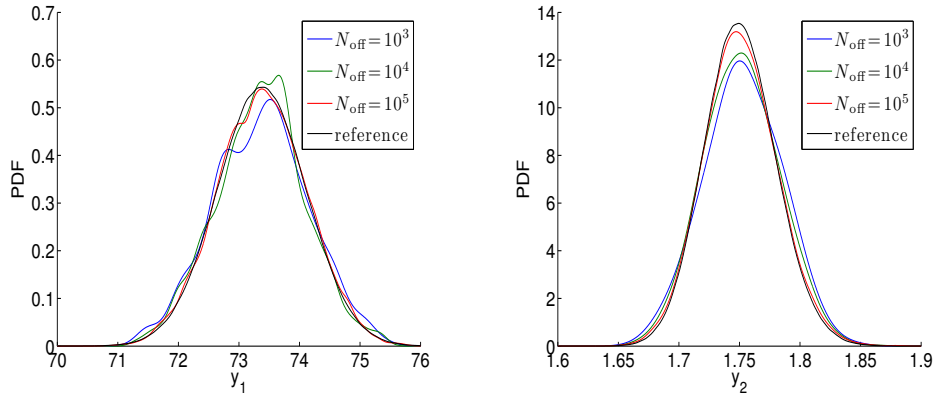

Figure 9: PDFs of the outputs of interest for a four-parameter test problem using the diffusion equation.

2.7 CUR Factorization

We have developed a new CUR matrix factorization based upon the Discrete Empirical Interpolation Method (DEIM) [SE14]. A CUR factorization provides a low rank approximate factorization of a given matrix $\mathbf{A} \in \mathbb{R}^{m\times n}$ that is of the form $\mathbf{A} \approx \mathbf{CUR}$ where $\mathbf{C} = \mathbf{A}(:,\mathbf{q}) \in \mathbb{R}^{m\times k}$ is a subset of the columns of $\mathbf{A}$ and $\mathbf{R} = \mathbf{A}(\mathbf{p},:) \in \mathbb{R}^{k\times n}$ is a subset of the rows of $\mathbf{A}$. The $k \times k$ matrix $\mathbf{U}$ is constructed to assure that $\mathbf{CUR}$ is a good approximation to $\mathbf{A}$. Assuming the best rank-k singular value decomposition (SVD) $\mathbf{A} \approx \mathbf{VSW}^T$ is available, the algorithm uses the DEIM points $\mathbf{q} = \text{DEIM}(\mathbf{V})$ and $\mathbf{p} = \text{DEIM}(\mathbf{W})$ to select the matrices $\mathbf{C}$ and $\mathbf{R}$.

This approximate factorization is nearly as accurate as the best rank k SVD approximation in the sense that

$$\|\mathbf{A} - \mathbf{CUR}\|_2 = O(\sigma_{k+1})$$

where σ_{k+1} is the first neglected singular value of $\mathbf{A}$.

The CUR factorization is an important tool for matrices built from large-scale data sets, in which case it offers two advantages over the SVD: when the data in $\mathbf{A}$ are sparse, so too are the $\mathbf{C}$ and $\mathbf{R}$ matrices, unlike the matrices of singular vectors; and the columns and rows that comprise $\mathbf{C}$ and $\mathbf{R}$ are representative of the data (e.g., sparse, nonnegative, integer valued, etc.). The following simple example, adapted from Mahoney and Drineas[2], illustrates the latter advantage. Suppose that $\mathbf{A} \in \mathbb{R}^{2\times n}$ has columns each of which are one of the forms

$$\begin{bmatrix} x_1 \\ x_2 \end{bmatrix}, \qquad \text{or} \qquad \frac{\sqrt{2}}{2}\begin{bmatrix} -1 & 1 \\ 1 & 1 \end{bmatrix}\begin{bmatrix} x_1 \\ x_2 \end{bmatrix},$$

where in both cases $x_1 \sim N(0,1)$ and $x_2 \sim N(0,4^2)$ are independent normal random samples. Thus the columns of $\mathbf{A}$ are drawn from two different multivariate normal distributions. Figure 10 shows that the two left singular vectors, though orthogonal by construction, fail to represent the true nature of the data; in contrast, the first two columns selected by the DEIM-CUR procedure give a much better overall impression of the data. While trivial in this two-dimensional case, one can imagine the utility of such approximations for high-dimensional data.

[2]CUR matrix decompositions for improved data analysis. *Proc. Nat. Acad. Sci.*, 106:697–702, 2009

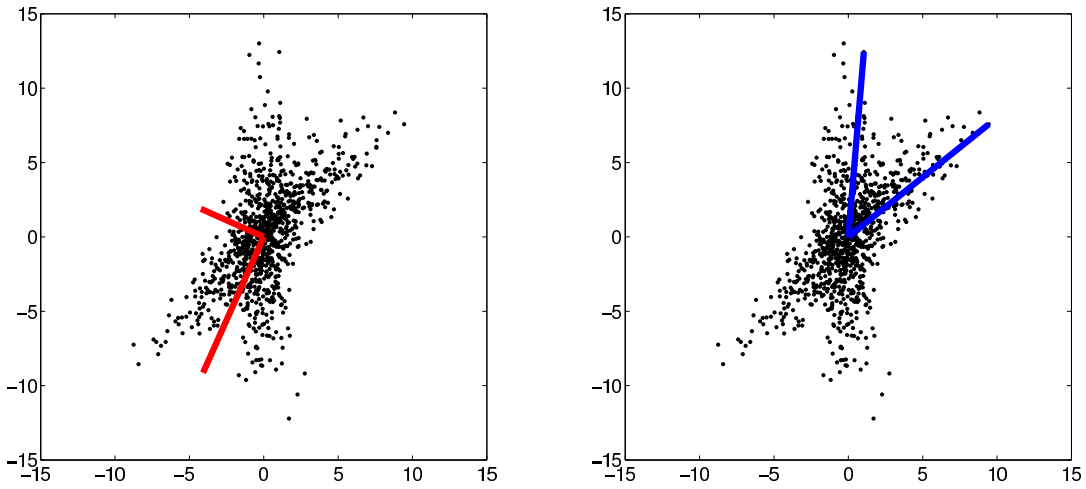

Figure 10: Comparison of singular vectors (left, scaled, in red) and DEIM-CUR columns (right, in blue) for a data set drawn from two multivariate normal distributions having different principal axes.

CUR-type factorizations had their origin in "pseudoskeleton" approximations[3] and pivoted, truncated QR decompositions[4]. Numerous prominent recent algorithms instead use *leverage scores*[5]. These algorithms all rely upon initially having a low rank SVD approximation. The error analysis of these algorithms is probabilistic in nature.

Our algorithm, based upon DEIM, is entirely deterministic and involves few (if any) parameters. We have developed an error analysis that applies to a broad class of CUR factorizations. We have also proposed a novel incremental QR algorithm for approximating the SVD. This approximate QR algorithm can also be applied to efficiently compute leverage scores if desired. The excellent performance of our new CUR factorization is illustrated on several examples. These results indicate that the DEIM-CUR approach generally provides far superior low rank approximations to the given data when compared to existing leverage score based methods.

The incremental low rank QR factorization has important consequences for POD based model reduction. Here, the given data $\mathbf{A} \approx \mathbf{VT}$ where the columns of $\mathbf{V}$ are mutually orthonormal and $\mathbf{T}$ is rectangular. Given a user specified tolerance tol, the procedure will automatically produce a rank k factorization that achieves $\|\mathbf{A} - \mathbf{VT}\| \leq tol\|\mathbf{T}\|$ where $\mathbf{V}$ is order $n \times k$ while $\mathbf{T}$ is order

[3] S. A. Goreinov, E. E. Tyrtyshnikov, and N. L. Zamarashkin. A theory of pseudoskeleton approximations. *Linear Algebra Appl.*, 261:1–21, 1997.

[4] G. W. Stewart. Four algorithms for the efficient computation of truncated QR approximations to a sparse matrix. *Numer. Math.*, 83:313–323, 1999.

[5] C. Boutsidis and D. P. Woodruff. Optimal CUR matrix decompositions, arXiv.cs.DS:1405.7910, 2014. P. Drineas, M. W. Mahoney, and S. Muthukrishnan. Relative-error *CUR* matrix decompositions. *SIAM J. Matrix Anal. Appl.*, pp. 844–881, 2008. M. W. Mahoney and P. Drineas, CUR matrix decompositions for improved data analysis. *Proc. Nat. Acad. Sci.*, 106:697–702, 2009. S. Wang and Z. Zhang, Improving CUR matrix decomposition and the Nyström approximation via adaptive sampling. *J. Machine Learning Res.*, 14:2729–2769, 2013.

$k \times n$. The algorithm is novel in that it only requires *one pass* through the data $\mathbf{A}$ and only requires a few columns of $\mathbf{A}$ to be in memory at any given step of the algorithm. This is ideal for POD based schemes since the high dimensional trajectory need not be stored.

To illustrate the performance of DEIM-CUR as compared to a leverage score algorithm, the following example builds a matrix $\mathbf{A} \in \mathbb{R}^{300,000 \times 300}$ having the form

$$\mathbf{A} = \sum_{j=1}^{10} \frac{1000}{j} \mathbf{x}_j \mathbf{y}_j^T + \sum_{j=11}^{300} \frac{1}{j} \mathbf{x}_j \mathbf{y}_j^T, \tag{3}$$

where $\mathbf{x}_j \in \mathbb{R}^{300,000}$ and $\mathbf{y}_j \in \mathbb{R}^{300}$ are sparse vectors with random nonnegative entries (in MATLAB, $\mathbf{x}_j = \texttt{sprand}(30000, 1, 0.025)$ and $\mathbf{y}_j = \texttt{sprand}(300, 1, 0.025)$). In this instantiation, about 18% of all entries of $\mathbf{A}$ are nonzero. The form (3) is not a singular value decomposition, since the vectors in $\{\mathbf{x}_j\}$ and $\{\mathbf{y}_j\}$ are not orthonormal; however, due to the sparsity of these vectors this decomposition suggests the structure of the SVD: the singular values decay like $1/j$, and with the first ten singular values weighted more heavily to give a significant drop between σ_{10} and σ_{11}.

Figure 11 compares the error $\|\mathbf{A} - C\mathbf{U}\mathbf{R}\|$ of the CUR approximation for DEIM-CUR to two methods based on leverage scores. For the first method, the rank-k approximation takes the k rows and columns that have the largest leverage scores computed using only the leading 10 left and right singular vectors; the second method is the same, but using all singular vectors. Both methods perform rather more poorly than DEIM-CUR, which closely tracks the optimal value σ_{k+1}. As seen in Figure 11, the DEIM-CUR approach delivers an excellent approximation, while selecting the rows and columns with the leading leverage scores does not perform nearly as well.

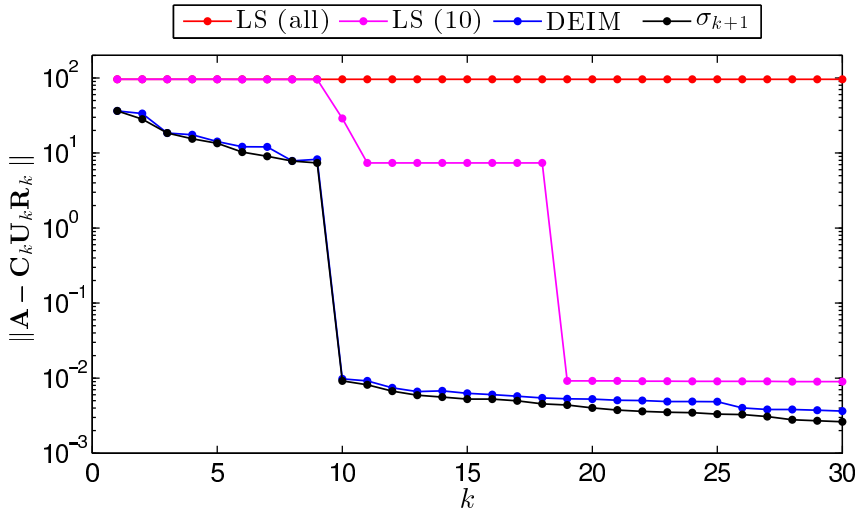

Figure 11: Accuracy of CUR approximations using k columns and rows, for DEIM-CUR and two leverage score strategies for the sparse, nonnegative matrix (3). "LS(all)" selects rows and columns having the highest leverage scores computed using all 300 singular vectors; "LS(10)" uses the leading 10 singular vectors.

Acknowledgment/Disclaimer

This work was sponsored (in part) by the Air Force Office of Scientific Research, USAF, under grants/contract numbers FA9550-12-1-0155, FA9550-12-1-0420. The views and conclusions contained herein are those of the authors and should not be interpreted as necessarily representing the official policies or endorsements, either expressed or implied, of the Air Force Office of Scientific Research or the U.S. Government.

References

[1] H. Antil, S. Hardesty, and M. Heinkenschloss, *Shape Optimization of Shell Structure Acoustics*, Technical Report, Department of Computational and Applied Mathematics, Rice University, 2014. Submitted (in review).

[2] H. Antil, M. Heinkenschloss, and D. C. Sorensen, *Application of the Discrete Empirical Interpolation Method to Reduced Order Modeling of Nonlinear and Parametric Systems*. In: Reduced Order Methods for Modeling and Computational Reduction, A. Quarteroni and G. Rozza (eds.). MS&A. Model. Simul. Appl., Vol. 9, 2014, pp. 101-136, Springer Verlag. doi: 10.1007/978-3-319-02090-7_4

[3] M. Bambach, M. Heinkenschloss, and M. Herty, *A Method for Model Identification and Parameter Estimation*. Inverse Problems, 2013, Vol. 29, No. 2, pp. 025009, doi:10.1088/0266-5611/29/2/025009.

[4] P. Benner, M. Heinkenschloss, J. Saak, and H. K. Weichelt, *Inexact low-rank Newton-ADI method for large-scale algebraic Riccati equations*. Max Planck Institute Magdeburg, Germany,Technical Report MPIMD/15-06, May 2015. Available at http://www.mpi-magdeburg.mpg.de/preprints.

[5] R. Carden and D.C. Sorensen, *Automating DEIM for Nonlinear Model Reduction*. Technical Report CAAM TR12-16, available on line at http://www.caam.rice.edu/tech reports.html,

[6] J. W. Gohlke, *Reduced Order Modeling for Optimization of Large Scale Dynamical Systems*, Masters Thesis, Department of Computational and Applied Mathematics, Rice University, 2013.

[7] D. P. Kouri, M. Heinkenschloss, D. Ridzal, and B. G. van Bloemen Waanders *A Trust-Region Algorithm with Adaptive Stochastic Collocation for PDE Optimization under Uncertainty*. SIAM Journal on Scientific Computing, 2013, Vol. 35, No. 4, pp. A1847-A1879, doi: 10.1137/120892362.

[8] D. P. Kouri, M. Heinkenschloss, D. Ridzal, and B. G. van Bloemen Waanders *Inexact Objective Function Evaluations in a Trust-Region Algorithm for PDE-Constrained Optimization*

under Uncertainty. SIAM Journal on Scientific Computing, 2014, Vol. 36, No. 6, pp. A3011-A3029, doi: 10.1137/140955665.

[9] Q. Liao and K. Willcox, *A Domain Decomposition Approach for Uncertainty Analysis*, SIAM Journal on Scientific Computing, 2015, Vol. 37, No. 1, pp. A103–A133, doi: 10.1137/140980508.

[10] B. Peherstorfer, D. Butnaru, K. Willcox and H.-J. Bungartz, *Localized Discrete Empirical Interpolation Method*, SIAM Journal on Scientific Computing, 2014, Vol. 36, No. 1, pp. A168–A192, doi: 10.1137/130924408.

[11] D.C. Sorensen and M. Embree, *A DEIM Induced CUR Factorization* CAAM Technical Report TR14-04, (2014).

[12] T. Takhtaganov, *High-Dimensional Integration for Optimization Under Uncertainty*, Masters Thesis, Department of Computational and Applied Mathematics, Rice University, 2015.

[13] D. Wirtz, D.C. Sorensen and B. Haasdonk, *A-posteriori Error Estimation for DEIM Reduced Nonlinear Dynamical Systems*, SIAM Journal on Scientific Computing, 2014, Vol. 36, No. 2, pp. A311–A338, doi: 10.1137/120899042.

1.

1. Report Type

Final Report

Primary Contact E-mail

Contact email if there is a problem with the report.

heinken@rice.edu

Primary Contact Phone Number

Contact phone number if there is a problem with the report

713-348-5176

Organization / Institution name

Rice University

Grant/Contract Title

The full title of the funded effort.

COLLABORATIVE RESEARCH: MODEL REDUCTION FOR NONLINEAR AND PARAMETRIC SYSTEMS WITH UNCERTAINTY

Grant/Contract Number

AFOSR assigned control number. It must begin with "FA9550" or "F49620" or "FA2386".

FA9550-12-1-0155

Principal Investigator Name

The full name of the principal investigator on the grant or contract.

Heinkenschloss, Matthias

Program Manager

The AFOSR Program Manager currently assigned to the award

Dr. Fariba Fahroo, Dr. Jean-Luc Cambier

Reporting Period Start Date

04/15/2012

Reporting Period End Date

04/14/2015

Abstract

This project has developed and analyzed new mathematical algorithms to substantially reduce the complexity of simulating and optimizing parametrically dependent systems and to support decision-making under uncertainty. Specifically, this research has advanced the state of the art in reduced order modeling based on projections and on the discrete empirical interpolation method (DEIM) for nonlinear systems, developed new adaptive sampling methods for optimization of systems with uncertain inputs, devised a domain decomposition based methods to systematically integrate the uncertainty propagation through components into uncertainty propagation through a systems composed of these components, established a so-called CUR factorization based on the DEIM that provides a low rank approximate factorization of a given large matrix with applications to POD model reduction and analysis of data. The feasibility of our algorithms was demonstrated on a number of problems with relevance to the Air Force.

Distribution Statement

This is block 12 on the SF298 form.

Distribution A - Approved for Public Release

Explanation for Distribution Statement

If this is not approved for public release, please provide a short explanation. E.g., contains proprietary information.

SF298 Form

Please attach your SF298 form. A blank SF298 can be found here. Please do not password protect or secure the PDF The maximum file size for an SF298 is 50MB.

SF298_Form_Rice_July10_2015.pdf

Upload the Report Document. File must be a PDF. Please do not password protect or secure the PDF . The maximum file size for the Report Document is 50MB.

FinalReport2015.pdf

Upload a Report Document, if any. The maximum file size for the Report Document is 50MB.

Archival Publications (published) during reporting period:

See attached report

Changes in research objectives (if any):

None

Change in AFOSR Program Manager, if any:

None

Extensions granted or milestones slipped, if any:

None

AFOSR LRIR Number

LRIR Title

Reporting Period

Laboratory Task Manager

Program Officer

Research Objectives

Technical Summary

Funding Summary by Cost Category (by FY, $K)

	Starting FY	FY+1	FY+2
Salary			
Equipment/Facilities			
Supplies			
Total			

Report Document

Report Document - Text Analysis

Report Document - Text Analysis

Appendix Documents

2. Thank You

E-mail user

Jul 12, 2015 17:52:55 Success: Email Sent to: heinken@rice.edu